

Received August 31, 2021; reviewed; accepted October 18, 2021

Study on screening performance and parameters optimization of double relatively independent vibrating screen

Zhanfu Li ^{1,2}, Yunxiao Hu ¹, Peiyu Jia ¹, Qiming Si ¹, Xin Tong ¹

¹ School of Mechanical and Automotive Engineering, Fujian University of Technology, Fuzhou, Fujian, 350118, China

² CSCC Strait Construction and Development Co. LTD, Fuzhou, Fujian, 350015, China

Corresponding author: Tongxin_hqu_fjut@163.com (X. Tong)

Abstract: In view of the existing double-layer linear vibrating screen, the screen surface inclination angle is basically parallel design. This paper puts forward a double-layer non-parallel and relatively independent vibrating screen. Experimental prototype of double-layer relatively independent vibrating screen under variable parameters was manufactured to verify the feasibility of simulations. This paper applied the single-factor tests to establish relationships between screening parameters of double-layer non-parallel and relatively independent vibrating screen and screening performance. What's more, the combination of screening parameters was optimized using the response surface method (RSM). The optimal combination after the round is as follow: vibration frequency 35 Hz, the angle of eccentric block 14.2°, the inclination of the upper screen 14.6° and the inclination of the lower screen 8.8°.

Keywords: RSM, non parallel, DEM-MBD co-simulation, relatively independent

1. Introduction

The vibrating screen is the main equipment for the classification of bulk materials. It is widely used in the construction industry, food and medicine and other industries that need to deal with bulk materials. Among them, the screen surface is the most important working part of the screening machine to bear the bulk material being screened and complete the screening process. At the same time, it is also an important factor affecting the performance of the screening process. Therefore, it is very important to use different research methods to increase the research on screening performance.

Screening performance has been a lot of work by some scholars. Qiong et al. (2018) studied the influence distribution law between the inclination of the three-degree-of-freedom vibrating screen surface and the screening efficiency. Li (2019) designed a new type of double-layer grain cleaning sieve. It uses an offset crank slider as the driving mechanism, and has the characteristics of non-parallelism and multiple degrees of freedom. Based on numerical analysis, Dong et al. (2017) studied the influence of mesh shape on the flow and stratification of particle groups. Davoodi et al. (2019) studied the changing law of the aperture in different materials, and the influence of the difference in aperture shape and screening medium material on the screening efficiency. Zhu and Sang (2010) used self-cleaning triangular hole screen and installation requirements to solve the problem in view of screen plugging and damage causes, effectively improving the screening performance of vibrating screen and reducing the particle plugging rate. Dong et al. (2009) simulated the screening process of linear and circular motion tracks of the banana screen surface according to the motion form of the screen surface, and concluded that compared with linear motion, circular motion could improve the screening performance of the banana screen better. Chen (2020) decomposes the elliptical vibration into linear vibration and circular vibration according to the vibration mode of the elliptical vibrating screen, and realized different vibration trajectories of screen by adjusting the proportion of long and short half axes of elliptical vibration trajectories.

Research methods of vibrating screens has been extensively studied by some scholars. Cleary et al. (2009ab) analyzed the movement characteristics of particle groups under the conditions of different accelerations, and carried out regular research on the performance indexes of the double-layer banana screening machine and made quantitative prediction. Kruggel-Emden and Elskamp (2014) studied the sieving related phenomena of non-spherical particles based on the discrete element method, and compared the experimental results with the simulation results. He, Wang and Liu (Liu, 2016; Hei, 2018; Wang, 2018) carried out dynamic simulation analysis on the screening machine based on the multi-rigid body dynamics method. It proves the feasibility and rationality of using ADAMS simulation software to analyze the screening machine, and provides theoretical reference for the development of the screening machine. Wang et al. (2018) used EALink to transmit data between ADAMS and EDEM, and obtained the contact force of granular media acting on the workpiece and the velocity between granular media and the workpiece through co-simulation.

To sum up, the current research on vibrating screen focuses on the screening performance and vibration characteristics, and few studies will consider the two comprehensively. In this paper, through the discrete element method and multi-body dynamics co-simulation, using multi-body dynamics to determine the motion form of vibrating screen surface, and through the discrete element method under such a motion form of screening parameters on the screening performance of two layers of relatively independent vibrating screen. The RSM was used to analyze the interaction between the screening parameters and to find the optimal combination of the screening parameters.

2. Simulation model

2.1. The simulation principle

2.1.1. The contact model in the DEM

The model is based on the work of Mindlin and Deresiewicz (1953). When the particle i with radius R_i is in elastic contact with the particle j with radius R_j , the normal overlap δ_n between the two particles is:

$$\delta_n = R_i + R_j - |\vec{r}_i - \vec{r}_j| \quad (1)$$

where \vec{r}_i and \vec{r}_j are the center position vector of particles i and j respectively. The mathematical formula between the normal contact force F_n and the normal overlap δ_n between particles i and j is as follows:

$$F_n = \frac{4}{3} E^* (R^*)^{\frac{1}{2}} \delta_n^{\frac{3}{2}} \quad (2)$$

where R^* is the equivalent radius, E^* is the equivalent Young's modulus. It can be solved by Eq. (3) and Eq. (4):

$$\frac{1}{R^*} = \frac{1}{R_i} + \frac{1}{R_j} \quad (3)$$

$$\frac{1}{E^*} = \frac{1-\gamma_i^2}{E_i} + \frac{1-\gamma_j^2}{E_j} \quad (4)$$

where γ_i^2 and γ_j^2 are the center position vector of particles i and j respectively. Additionally, there is a damping force, F_n^d given by:

$$F_n^d = -2 \sqrt{\frac{5}{6}} \beta \sqrt{K_n m^*} v_n^{rel} \quad (5)$$

$$K_n = 2E^* (R^* \delta_n)^{\frac{1}{2}} \quad (6)$$

$$m^* = \frac{m_i m_j}{m_i + m_j} \quad (7)$$

$$v_n^{rel} = (\vec{v}_i - \vec{v}_j) \cdot \vec{n} \quad (8)$$

where K_n is the normal stiffness, m^* is the reduced mass, v_n^{rel} is the normal component of the relative velocity, \vec{v}_i and \vec{v}_j are the speed of particles i and j respectively. The solution formula between the tangential force F_t and the tangential overlap δ_t between particles i and j is as follows:

$$F_t = -K_t \delta_t \quad (9)$$

$$K_t = 8G^*(R^*\delta_t)^{\frac{1}{2}} \quad (10)$$

$$\frac{1}{G^*} = \frac{1-\gamma_i^2}{G_i} + \frac{1-\gamma_j^2}{G_j} \quad (11)$$

where K_t is the tangential stiffness, G^* is the equivalent shear modulus. Additionally, tangential damping is given by:

$$F_t^d = -2\sqrt{\frac{5}{6}}\beta\sqrt{K_t m^*}v_t^{rel} \quad (12)$$

where v_t^{rel} is the relative tangential velocity.

2.1.2. The basic principle of ADAMS co-simulation interface

The combined simulation of discrete element method and multi-rigid body dynamics is widely used in the numerical simulation calculation of the interaction between bulk materials and mechanical parts. During co-simulation, a six-degree-of-freedom spatial force "gravity" must be placed on each component participating in the coupling, that is, a gravity is placed on each interaction point. And gravity must react on the ground (the JFLOAT mark must be on the ground). The RM marking point must be located on the ground, and its position must be consistent with the ground origin and parallel to the ground. The position of the I marking point must be consistent with the position of the interaction point (the position of the geometric CM marking point in the EDEM model must be the same), and it must be parallel to the ground. The interaction point model of EDEM-ADAMS is shown in Figure 1.

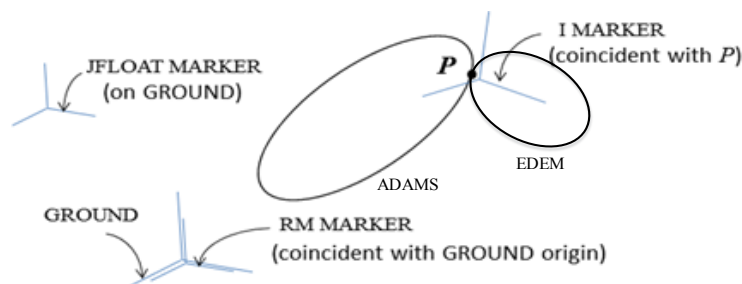


Fig. 1 The interaction point model of EDEM-ADAMS

EALink is used as an interface for interacting motion data in EDEM and ADAMS. First, EDEM can be used to calculate the force of particles acting on mechanical parts and ADAMS can be used to calculate the motion force caused by bulk materials. Finally, the particle force and mechanical parts can be passed through EALink. The motion data is transmitted interactively at each time step in EDEM and ADAMS. On the one hand, it provides more complex and real movements for the mechanical parts of bulk material handling equipment; on the other hand, the force generated by the passive movement of the particle group will affect the mechanical parts of the equipment, causing the mechanical parts to vibrate or flip; For EALink, it makes the above simulation process very simple.

2.3. Simulation model and conditions

Due to the complexity of the structure of the vibrating screen, a simplified DEM model of the vibrating screen is presented in Fig. 2, which mainly includes screen box, particle factory, upper and lower screen. Particle factory is the generation of screened particle groups in discrete element software that can be defined by the user's own needs, such as the generation of particles with different particle sizes through normal distribution. Screen surface is the core mechanical structure of vibrating screen components, it makes the sieve particle group in the process of screening classification, the complex motion of the screen surface can be solved by applying various basic motion functions of the screen surface in the software. In this paper, through the combination of EDEM and ADAMS, the motion of screen mesh in ADAMS is transferred to EDEM, that is, the motion of screen mesh in EDEM is controlled by ADAMS, as shown in Fig 2b. The resultant force (particle force, contact force) received by the particles in the screening process is related to the physical properties and motion speed of the particles, which makes

the particles have certain motion characteristics. The material properties and collision coefficients of the model are shown in Table 1 and Table 2.

The granular materials generated by the bimodal normal distribution with the mean diameter of 1 and 2 mm were used respectively. The total number of particles is 1000 in every simulation, and the generation rate is 13333 particles s⁻¹.

Table 1. The material properties in EDEM model

Material properties	Poisson's ratio	Shear modulus/ Pa	Density/kg/m ³
Particles	0.3	2.3e+07	2678
Screen	0.29	7.992e+10	7861

Table 2. The collision coefficients in EDEM model

collision coefficients	Coefficient of restitution	Coefficient of static friction	Coefficient of rolling friction
Particle-particle	0.1	0.545	0.01
Particle-geometry	0.2	0.5	0.01

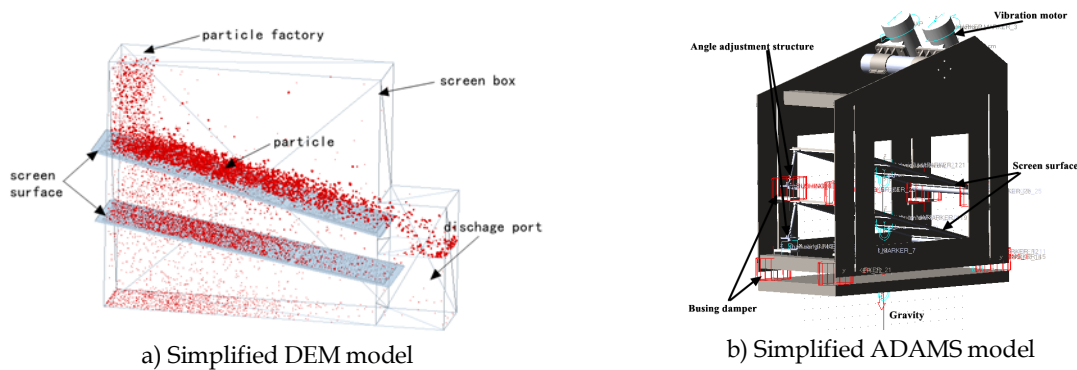


Fig. 2. Simulation model

2.4. Screening efficiency

The ultimate goal of screening is to classify a batch of bulk materials according to the size of the sieve holes on the screen. In the ideal sieving process, the fine particles smaller than the sieve hole size all fall under the sieve, but in fact, due to various factors, some of the sieved particles remain on the sieve surface, resulting in ineffective sieving. In this paper, the screening efficiency per unit time is selected as the evaluation index of screening performance. The screening efficiency per unit time is the difference between the screening efficiency of target particles and non-target particles under unit time, screening efficiency per unit (Li et al., 2015; Lan, 2016; Li, 2016; Li and Tong, 2016; Li et al, 2018):

$$\mu = \frac{\left(\frac{m_{<r}^L}{m_{<r}} - \frac{m_{>r}^L}{m_{>r}} \right) \times 100\%}{t} \quad (13)$$

where $m_{<r}^L$, $m_{>r}^L$ are the mass of particles whose diameters are smaller than and bigger than the separation particle size r in the undersized material, respectively, $m_{<r}$ and $m_{>r}$ are the mass of particles whose diameters are smaller than and bigger than the separation particle size r in the material. t is the time of the screening process. In this paper, screening efficiency is used instead of unit time screening efficiency.

2.5. The experimental prototype

In Fig. 3, the two-layer relatively independent vibrating screen experimental prototype, two vibration motors are connected with the screen body through the motor seat. Change the included angle α of two

eccentric blocks to adjust the excitation force stepless; The speed of the two vibration motors is controlled by the frequency converter to achieve stepless adjustment of the speed; The change of the screen surface installation angle through the screen surface angle adjustment structure on the screen body sliding up and down and rotation to adjust the screen surface angle from the level to 30 degrees; Through the observation window, the motion state of the screened particle group on the screen can be observed. At the same time, high-speed camera can be used to film the motion state of the screened particle group and analyze the dispersion, stratification and penetration of the screened particle group. The aperture sizes of braided screens used in this paper are 1mm and 2mm respectively.

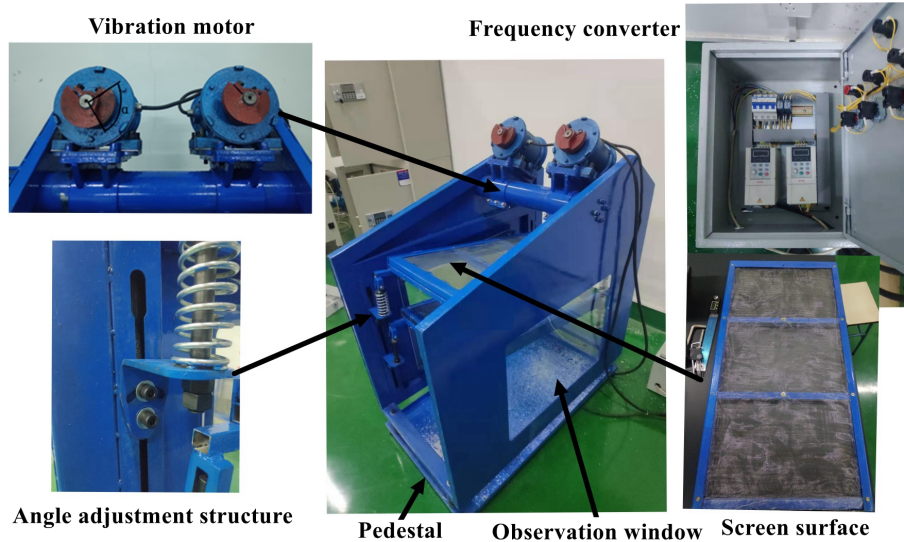


Fig. 3. Experimental prototype

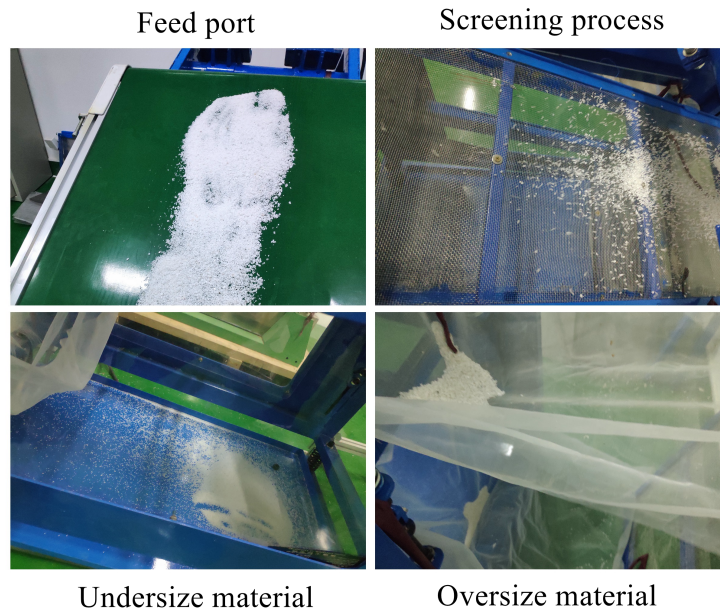


Fig. 4. Experimental process

To verify the reliability of the simulation test, the test prototype of the double-layer relatively independent vibrating screen was used to study the single vibration parameters. The single factor experiments of 5 groups of vibration frequencies were designed to study the relationship between vibration frequency and screening efficiency per unit time, respectively: vibration frequency 30Hz, 35Hz, 40Hz, 45Hz and 50Hz. The experimental data results were plotted as shown in Fig. 5. Meanwhile,

the experimental data results under the test prototype were compared with the simulation test data results under the same parameters.

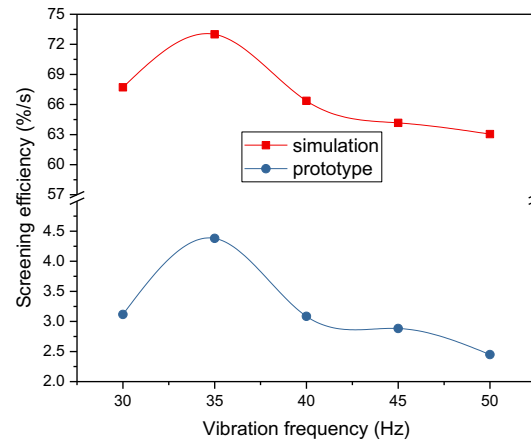


Fig. 5. Comparison between co-simulation and test prototype

As can be seen from Fig. 5, when a single vibration parameter changes, there is a certain difference between the simulation test of the two-layer relatively independent vibrating screen and the prototype test in numerical value, but the overall trend of change is consistent.

3. Results and discussion

3.1. Single-factor tests

In this paper, four screening parameters, such as vibration frequency, including angle of eccentric block and the inclination of upper and lower screen surfaces, are studied by using ADAMS and EDEM under the condition of MBD-DEM co-simulation. A single factor test was established to study the effects of screening parameters on screening performance. The changes of test design parameters are shown in Table 3.

Table 3. Single factor test parameters

	Vibration frequency	Angle of eccentric block	Upper screen surface inclination	Lower screen surface inclination
First group	30,35,40,45,50	10	15	15
Second Group	35	10,30,50,70,90	15	15
Third group	35	10	9, 12,15,18,21	15
Fourth group	35	10	15	9, 12,15,18,21

3.1.1. Influence of screening parameters on screening performance

The vibration frequency has an important effect on the activity of the particles on the screen surface, and also affects the looseness, delamination and penetration of the particles on the screen surface. Fig. 6a shows the influence of variation in the vibration frequency on the screening efficiency. It can be seen from Fig. 6a that the vibration frequency had an important effect on the screening efficiency. As vibration frequency increased from 30 to 35Hz, the screening efficiency first increased and then decreased. When the vibration frequency was 35Hz, the screening efficiency reached the maximum with a value of 0.7300. Generally, when the vibration frequency is greater than 35Hz, as the vibration frequency increases, the beat times of the particles and the screen surface will increase, which reduces the penetration probability and thus the screening efficiency. When the vibration frequency is less than 35Hz, with the increase of vibration frequency, the particles on the screen surface is easier to lose, stratified and through the screen, so that the screening efficiency increases accordingly.

The angle of the eccentric block mainly affects the magnitude of the vibration force, thus affecting the amplitude. The larger the angle of the eccentric block makes the particles adhere to the surface of

the screen. This result in particles that are not conducive to lose stratification. Fig. 6b shows the influence of variation in the angle of eccentric block on the screening efficiency. As shown in Fig. 6b, the angle of eccentric block had a significant effect on the screening efficiency. The screening efficiency tended to decrease with increased in the angle of eccentric block. This is because the greater the angle of the eccentric block, the greater the contact time between the particles and the screen surface, so that the particles are lot easy to disperse and stratify, resulting in the reduction of screening efficiency.

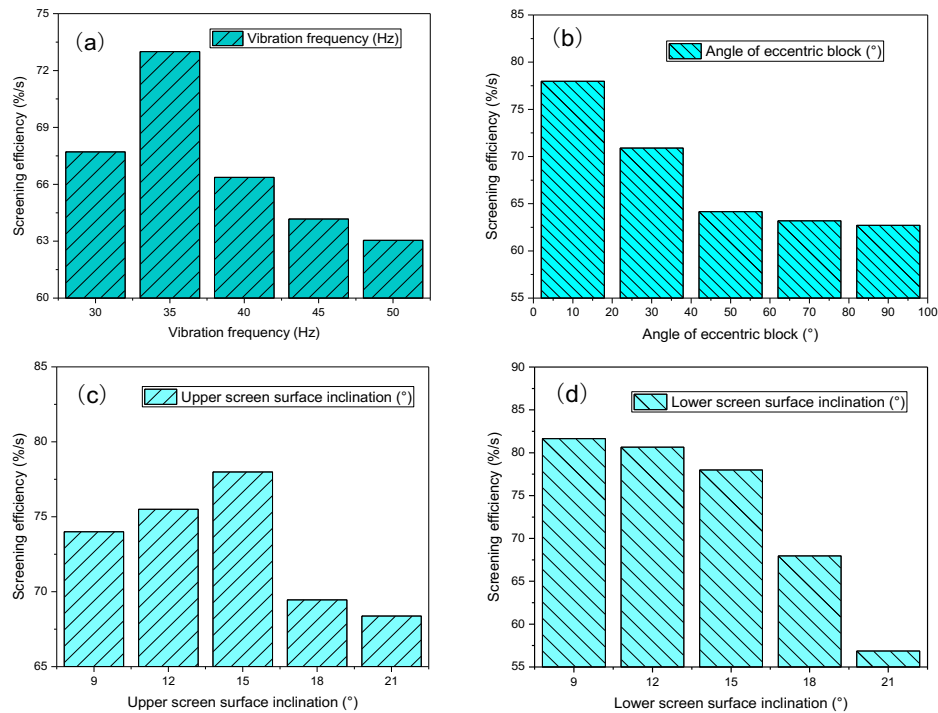


Fig. 6. The influence of screening parameters on screening efficiency

The inclination of the screen surface affects the throwing intensity of the particles on the screen surface, which is mainly manifested as the energy of the motion of the particle group on the screen surface. The angle of the screen surface determines the velocity of the particles along the direction of the screen length, and then affects the screening time and screening efficiency per unit time. Fig. 6c and d shows the influence of variation in the inclination of upper and lower screen surface on the screening efficiency. It can be clearly seen from Fig. 6c and d, the inclination of upper and lower screen surface had an important effect on the screening efficiency. From Fig. 6c and d, it can be seen that the variation trend of screening efficiency does not increase with increase in the inclination of screen surface. When the inclination angle of the upper and lower screen surface is 15° and 9° respectively, the screening efficiency reaches the maximum. The screening efficiency first increases and then decreases in the upper screen, but decreases slowly with the angle of screen surface in the lower screen.

For the change of the inclination of upper and lower screen surface, there are 5 groups of changes: 6° , 3° , 0° , -3° and -6° . As can be seen from the figure, with the change of inclination from 6° to -6° in the upper screen, the screening efficiency firstly increases and then decreases. However, with the angle of screen surface from 6° to -6° , the screening efficiency decreases monotonically with increase in the inclination of lower screen surface. As can be seen from the figure, when the upper and lower layers have different inclination, the value of screening efficiency is larger than that of the upper and lower layers with the same inclination.

3.2. RSM experiment

3.2.1. Experimental design

Based on the single-factor experimental results, the best range of screening parameters was determined. On this basis, the RSM test on the influence of screening parameters and screening efficiency was

established in this section. Therefore, to select a better level, RSM was used to carry out combinatorial optimization of screening parameters.

Experiments of four factors and three levels were designed. The experimental design was carried out using the Design Expert software (version-12). The settings of factors and levels are shown in Table 4.

In accordance with the design in Table 4, the samples were fabricated and the screening efficiency was tested. The results are shown in Table 5.

Table 4. Factors and levels of RSM

Factors	Codes	Levels		
		-1	0	1
Vibration frequency /Hz	A	33	35	37
Angle of eccentric block /°	B	10	15	20
Upper screen inclination /°	C	14	15	16
Lower screen inclination /°	D	8	9	10

Table 5. Experimental results of RSM

No.	Experimental values				Response values
	A	B	C	D	Screening efficiency
1	35	10	14	9	78.1791
2	33	15	15	8	78.0381
3	35	20	15	8	77.5631
4	35	10	15	8	77.8441
5	37	20	15	9	72.0251
6	35	15	14	10	78.5778
7	35	15	15	9	82.6321
8	35	15	16	8	72.7429
9	33	15	15	10	73.7234
10	33	10	15	9	78.881
11	33	15	16	9	70.8311
12	37	15	15	10	71.8026
13	35	15	15	9	83.0273
14	35	15	15	9	83.3115
15	35	15	15	9	82.6678
16	33	15	14	9	78.627
17	35	20	14	9	78.6676
18	35	15	15	9	81.608
19	35	10	16	9	75.7884
20	35	15	14	8	79.7745
21	37	15	15	8	77.5144
22	33	20	15	9	76.3697
23	35	20	16	9	65.5531
24	35	15	16	10	65.8415
25	37	15	14	9	78.5969
26	37	10	15	9	78.8869
27	35	20	15	10	67.8951
28	35	10	15	10	78.4641
29	35	15	15	9	83.1273
30	37	15	16	9	68.9428

3.2.2. Establishment and significance test of RSM model

Polynomial fitting was performed on the data in Table 5. A quaternary quadratic regression equation was used to describe the relationship between screening parameters and screening efficiency. The regression equation obtained was expressed as:

$$Y = 82.73 - 0.7251A - 2.5B.4039C - 2.26D - 1.09AB - 0.4645AC - 0.3493AD - 2.68BC - 2.57BD - 1.43CD - 3.38A^2 - 3.15B^2 - 4.90C^2 - 3.94D^2 \quad (R_{Adj}^2 = 0.9816) \quad (14)$$

where, A is the vibration frequency, B is the included angle of eccentric block, C is the upper screen inclination, D is the angle of lower screen, Y is the response value of screening efficiency. R_{Adj}^2 represents the fitting degree of the regression equation, and the value of X is close to 1, indicating that the fitting degree of the regression equation is better. The analysis results of the regression model are shown in Table 6.

As shown in Table 6, the F-value of 111.75 and the P-value of model < 0.0001 implied the model was significant. The F-value of the lack of fit is 1.41 and the P-value of 0.3684 > 0.05, implying it was not significant relative to the pure error. Therefore, the model fitted the data well and was applied to describe the relationship between screening parameters and screening efficiency.

The P-values of A-A, B-B, C-C, D-D, AB, BC, BD, CD, A2, B2, C2 and D2 were all < 0.05, indicating that the influence of both screening parameters on screening efficiency were statistically significant. In addition, other screening parameters are more significant than that of vibration frequency.

Table 6. Analysis of variance of regression model

Source	Sum of Squares	df	Mean Square	F-value	p-value	
Model	741.54	14	52.97	111.75	< 0.0001	significant
A-A	6.31	1	6.31	13.31	0.0024	
B-B	74.85	1	74.85	157.92	< 0.0001	
C-C	231.64	1	231.64	488.73	< 0.0001	
D-D	61.53	1	61.53	129.81	< 0.0001	
AB	4.73	1	4.73	9.98	0.0065	
AC	0.8632	1	0.8632	1.82	0.1972	
AD	0.4880	1	0.4880	1.03	0.3264	
BC	28.75	1	28.75	60.66	< 0.0001	
BD	26.46	1	26.46	55.83	< 0.0001	
CD	8.14	1	8.14	17.16	0.0009	
A ²	78.42	1	78.42	165.45	< 0.0001	
B ²	67.91	1	67.91	143.27	< 0.0001	
C ²	164.39	1	164.39	346.83	< 0.0001	
D ²	106.39	1	106.39	224.46	< 0.0001	
Residual	7.11	15	0.4740			
Lack of Fit	5.25	10	0.5253	1.41	0.3684	not significant
Pure Error	1.86	5	0.3713			
Cor Total	748.65	29				

3.2.3. Analysis of RSM model

3.2.3.1. Interaction between vibration frequency and the angle of eccentric block

Fig. 7 shows the influence of vibration frequency and angle of eccentric block on the screening efficiency. When the inclination of the upper and lower screen surfaces are at zero level and the angle between the eccentric blocks is at a high level, the screening efficiency increases first and then decreases with the increase of vibration frequency. Its variation range is lower than that of the low level. With the increase

of vibration frequency, the beat times of particle group on the screen surface increase. This makes it easier for the particles to be dispersed and stratified. But when the vibration frequency is too large, it will reduce the probability of penetration, so that the screening efficiency decreases. When the vibration frequency is too small, the particle group is not easy to disperse and stratified, resulting in particle plugging hole and the reduction of screening efficiency. Fig. 7(b) shows the contour line diagram of the response surface. The extreme values of screening efficiency appeared in the red region at approximately the vibration frequency of 34 Hz ~36 Hz and the angle between eccentric blocks of 10° ~ 16° .

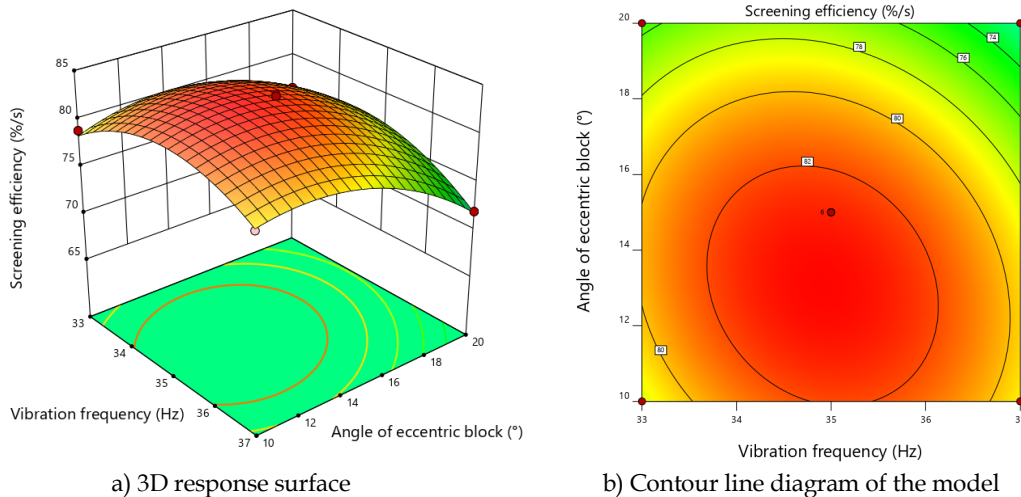


Fig. 7. Interaction between vibration frequency and the angle of eccentric block

3.2.3.2. Interaction between the angle of eccentric block and the inclination of upper and lower screen surfaces

Fig. 8 shows the influence of the angle of eccentric block and the inclination of the upper screen surfaces on the screening efficiency. When vibration frequency and the angle of the lower screen surface are at zero level and the angle of the eccentric block is at a low level, the screening efficiency first increases and then decreases with the increase of the angle of the upper screen surface. Its variation range is higher than that of the high level. The main reason for this phenomenon is that with the increase of the upper screen surface inclination, the residence time of particles on the screen surface decreases. It makes particles flow out of the screen surface more quickly, thus reducing the screening efficiency. Fig. 8(b) shows the contour line diagram of the response surface. The extreme values of screening efficiency appeared in the red region at approximately the inclination of the upper screen surface is 14° ~ 15.5° and the angle of the eccentric block is 10° ~ 20° .

Fig. 9 shows the influence of the angle of eccentric block and the inclination of the lower screen surfaces on the screening efficiency. When vibration frequency and the upper screen surface inclination are at zero level, and the lower screen surface inclination is at a high level, the screening efficiency first increases and then decreases with the increase of the angle of the eccentric block. The variation range of the inclination of lower screen surface is relatively gentle at a low level. The main reason for this phenomenon is that with the increase of the angle of the eccentric block, the vibration force is the smaller. This makes it drop the jump height of particles on the screen surface, so that the screening efficiency falls. But when the angle of the eccentric block is too large, it will cause the particle to block the hole and reduce the screening efficiency. According to Fig. 9(b), the extreme values of screening efficiency appeared in the red region at approximately the angle of the lower screen surface is 8° ~ 9.5° and the angle of the eccentric block is 10° ~ 18° .

3.2.3.3. Interaction between the inclination of upper and lower screen surfaces

Fig. 10 shows the influence of the inclination of upper and lower screen surfaces on the screening efficiency. When vibration frequency and the angle of eccentric block is at zero level, and the inclination of upper screen surface is at a low level, the screening efficiency increases first and then decreases with

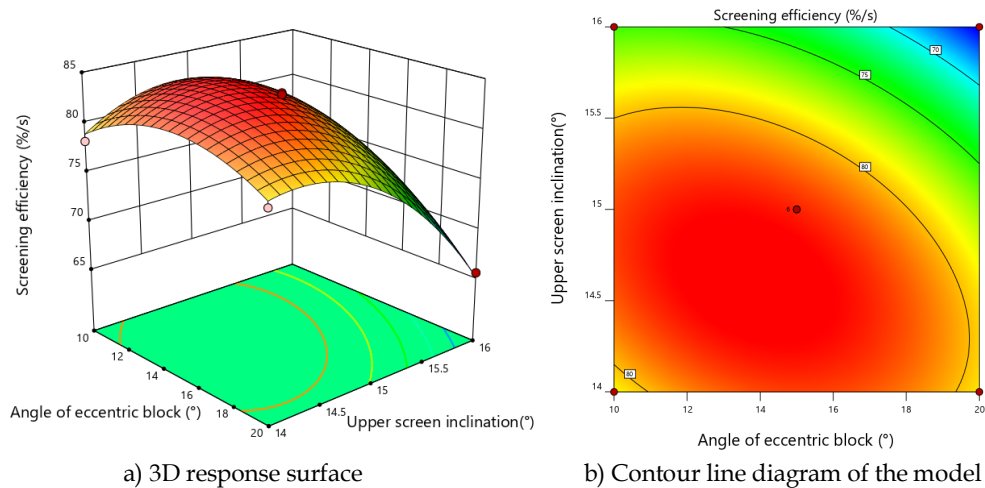


Fig. 8. Interaction between the angle of eccentric block and the angle of the upper screen surface

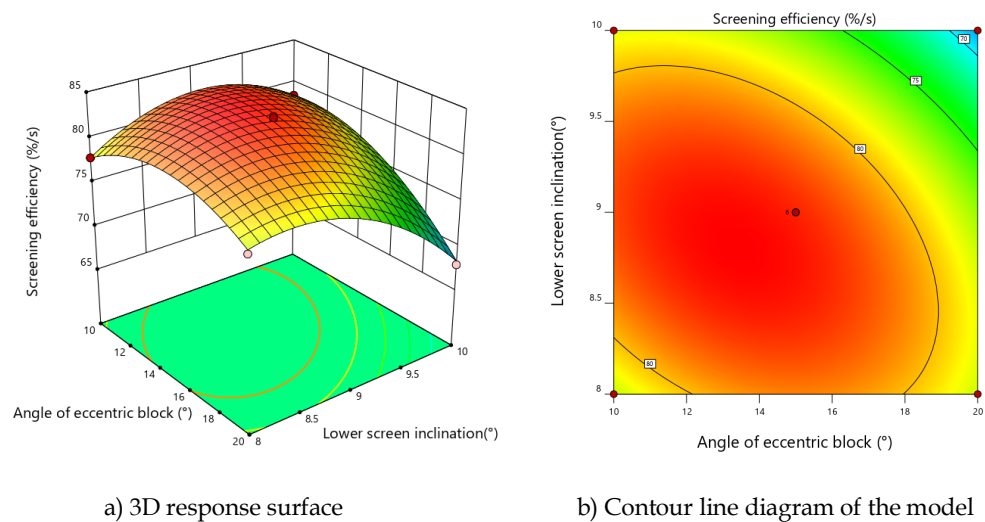


Fig. 9. Interaction between the angle of eccentric block and the angle of lower screen surface

the increase of the inclination angle of lower screen surface. The variation range is higher than that of the high level. This phenomenon is mainly that with the increase of the angle of the lower screen surface, the screen surface spacing between the upper and lower screen surface decreases. Meanwhile, the angle of screen surface is increases. The phenomenon makes the contact time between the particles and the screen surface become smaller, thus making the screening efficiency increase. But the screen surface spacing is too small and the screen surface angle is too large, so that the particles are not easy to disperse and stratified. As can be seen from Fig. 10(b), the extreme values of screening efficiency appeared in the red region at approximately the angle of the upper screen surface of $14^{\circ}\sim 15.5^{\circ}$ and the inclination of the lower screen of $8^{\circ}\sim 9.55^{\circ}$.

In conclusion, the variation trend of the influence law of screening parameters on screening efficiency is firstly increased and then decreased. The extreme values of screening efficiency appeared in the red region at approximately vibration frequency of 34 Hz ~36 Hz, the angle of the eccentric block of $10^{\circ}\sim 16^{\circ}$, the inclination of the upper screen of $14^{\circ}\sim 15.5^{\circ}$, and the inclination of the lower screen of $8^{\circ}\sim 9.55^{\circ}$.

3.2.4. Optimization and verification

The extreme value of screening efficiency was calculated by applying the regression Eq. (14), and the stagnation point within the response surface was determined to be 4.905 Hz, 14.197° , 14.621° , 8.836° . The screening efficiency was the highest when vibration frequency was 34.905 Hz, the angle of eccentric

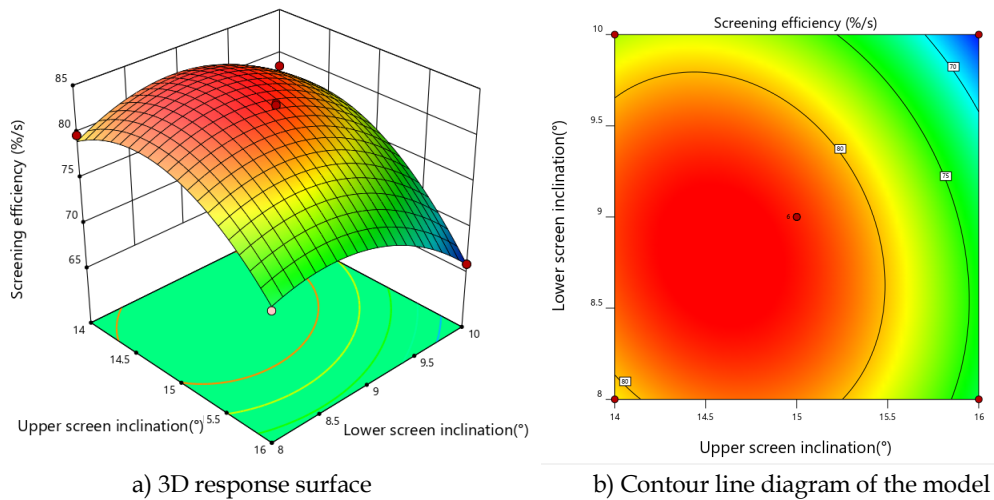


Fig. 10 Interaction between the inclination of upper and lower screen surfaces

block was 14.197° , the inclination of the upper screen was 14.621° and the inclination of the lower screen was 8.836° respectively. Substituting 34.905 Hz, 14.197° , 14.621° , 8.836° into the regression equation, the screening efficiency predicted using RSM was 83.964%/s.

To verify the accuracy of the RSM prediction, a comparative test was designed according to the optimized values after rounding. The effective screening efficiency obtained was 84.125%/s, which was higher than the predicted value of 83.964%/s, indicating that the combination of screening parameters is desirable.

4. Conclusions

From this work, we can get the following conclusions:

1) Through single factor test, the influence of screening parameters on screening performance of vibrating screen is studied, and the screening performance is firstly increased and then decreased with the increase of vibration parameters.

2) Through variance analysis of regression model, it is found that the screening parameters and the interaction between the parameters have a significant effect on the screening performance.

3) A quaternary quadratic regression equation was used to fit the co-simulation data, and a suitable response surface was established to describe the relationship between screening parameters on screening efficiency. The optimal combination is as follows vibration frequency 34.905 Hz, the angle of eccentric block 14.197° , the inclination of the upper screen 14.621° and the inclination of the lower screen 8.836° , screening efficiency 83.964%/s.

4) The screening performance of double-layer vibrating screen is studied regularly by DEM and MBD co-simulation, and the reliability of this method is verified by real experiment, which provides a new idea for the parameter optimization of vibrating screen.

In summary, this methodology could be applied to the research of vibrating screen. Additionally, this has certain guiding significance to the design and manufacture of vibrating screen.

Acknowledgements

The authors gratefully acknowledged the support from the Program for scientific and technological innovation flats of Fujian Province (2020-GX-16). Fujian Natural Science Foundation (2020J01870). No part of this paper has published or submitted elsewhere. The authors declared that they have no conflicts of interest to this work. All authors have seen the manuscript and approved to submit to your journal.

References

QIONG, L., GONG, D., LING, Q., LI, S., 2018. *Potassium Ore Particles Separation Efficiency Analysis in 3-DOF*

- Vibrating Screen Based on DEM*, in International Conference on Sensing, Diagnostics, Prognostics, and Control (SDPC), 376-379. <https://doi.org/10.1109/SDPC.2018.8664940>.
- LI, R., 2019. *Design and Experiment of Double Non Parallel Vibrating Screen*, Northeast Agricultural University.
- DONG, K., ESFANDIARY, A.H., YU, A.B., 2017. *Discrete particle simulation of particle flow and separation on a vibrating screen: Effect of aperture shape*, Powder Technology, 314, 195-202.
- [DAVOODI, A., BENGTTSSON, M., HULTHEN, E., EVERTSSON, C.M., 2019. *Effects of screen decks' aperture shapes and materials on screening efficiency*, Minerals Engineering, 139, 105699.
- ZHU, J.H., SANG, X.C., 2010. *The reasons causing clogging and damage of wire screen and its solution*, (in chinese), Mining Machinery, 38(1), 104-106.
- DONG, K.J., YU, A.B., BRAKE, I., 2009. *DEM simulation of particle flow on a multi-deck banana screen*, Minerals Engineering, 22(11), 910-920.
- CHEN, Z.Q., 2020. *Numerical Investigation and Performance Optimization of Elliptical Vibrating Screen*, Huaqiao University.
- CLEARY, P.W., SINNOTT, M.D., MORRISON, R.D., 2009a. *Separation performance of double deck banana screens – Part 1: Flow and separation for different accelerations*, Minerals Engineering, 22(14), 1218-1229.
- CLEARY, P.W., SINNOTT, M.D., MORRISON, R.D., 2009b. *Separation performance of double deck banana screens – Part 2: Quantitative predictions*, Minerals Engineering, 22(14), 1230-1244.
- KRUGGEL-EMDEN, H., ELSKAMP, F., 2014. *Modeling of Screening Processes with the Discrete Element Method Involving Non-Spherical Particles*, Chemical Engineering & Technology, 37(5), 847-856.
- LIU, Q., 2016. *Study on 3-DOF Hybrid Vibration Screen and Particle Motion Law in Screen Surface*, AnHui University of Science and Technology.
- HEI, X., 2018. *Design and study of multidimensional shavings swinging screen*, AnHui University of Science and Technology.
- WANG, J., 2018. *Discrete element analysis of tamping coking coal and structural study of tamping machine*, Zhejiang University of Technology.
- WANG, X.Z., YANG S.Q., LI, W.H., WANG, Y.Q., 2018. *Vibratory finishing co-simulation based on ADAMS-EDEM with experimental validation*, The International Journal of Advanced Manufacturing Technology, 96(1-4), 1175-1185.
- MINDLIN, R.D., DERESIEWICZ, H., 1953. *Elastic sphere in contact under varying oblique forces*, J. Appl. Mech., 20(3), 327-344.
- LI, Z.F., TONG, X., ZHOU, B., WANG, X.Y., 2015. *Modeling and parameter optimization for the design of vibrating screens*, Minerals Engineering, 83, 149-155.
- LAN, M.T., 2016. *The Research of Stratification Mechanism of Vibration Screen based on Composite Motion of Swing and Translation*, Huaqiao University.
- LI, Z.F., 2016. *Theoretical research and Parameters optimization of Vibrating screening Based on composite motion of Translation and Swing*, Huaqiao University.
- LI, Z. F, TONG, X., 2016. *Modeling and parameter optimization for vibrating screens based on AFSA-SimpleMKL*, " Chinese Journal of Engineering Design, 23(02), 181-187.
- LI, Z.F., TONG, X., ZHOU, B., GE, X.L., LING, J.X., 2018. *Design and Efficiency Research of a New Composite Vibrating Screen*, Shock and Vibration, 2018, 1-8.